On the nature of electromagnetic pulse emission generated by short-pulse lasers and the possible mitigation methods

P. Rączka[1], M. Rosiński[1], P. Tchórz[1], D. Terwińska[1], M. Szymański[1], K. Tomaszewski[1]
[1] *Institute of Plasma Physics and Laser Microfusion, Warsaw, Poland*

One of the side effects of high-intensity laser-target interactions under conditions typical for laser-induced proton acceleration is an undesirable strong emission of electromagnetic pulses (EMP) in the MHz to multi-GHz frequency range, as was recently reviewed in [1]. The physical origin of these signals is clear, they are related to the creation and propagation of hot electron bunches, which leads to the electric polarization of the target that initiates strong neutralization currents, than in turn lead to EMP emissions with target support acting as an antenna; other sources include charge separation radiation [2], escaping electrons and accelerated ion striking the chamber walls, and currents induced by x-ray photoelectrons. However, quantitative EMP estimates are challenging [3]. This comes from the fact that EMP effect combines kinetic particle aspects with electromagnetic circuit aspects, and there are only few codes that can handle that. Furthermore, EMP effect involves multitude of disparate length scale – from laser-plasma interaction scale (few µm), target size (few mm), stalk size (few cm), to the size of interaction chamber (~1 m) – and a wide range of time scales – tens of fs to few ps for laser-target interaction, 100's of ps for target neutralization time, to 100's of ns for EMP reverberations inside the interaction chamber. In this note we report on a numerical study of EMP generation and mitigation performed in a simplified approach. The aim of our study was to compare EMP emission from foils placed on metal stalks, dielectric stalks, and foils placed in the so-called birdhouse targets designed to facilitate the EMP mitigation [4].

For a simplified computation of EMP we restricted simulations to a small region in a direct vicinity of the target and to a short time interval (few ns) after the laser-target interaction. Secondly, we did not attempt to simulate directly the fast electron emission from the target, but instead made some assumptions about the escaping electrons using the very simplified but very tractable model of [5] as a guide. To compute the electromagnetic fields in the vicinity of the target we then used a commercial CST Studio Suite package which has the required combined circuit and Particle-in-Cell capability. The reverberations of thus computed original signal are likely to constitute the dominant part of the EMP recorded inside the interaction chamber. We simulated three types of the targets: a foil on a Cu stalk; a foil on a dielectric stalk, and the so-called birdhouse target [4].

In order to formulate input conditions for CST Studio Suite package we ran the ChoCoLaT2 code [5] for the conditions of our experimental setup: 45 fs pulse duration, 290 mJ pulse energy on target, 12 μm laser spot size. We used the data on maximum laser-accelerated proton energies to estimate the laser-to-fast-electron conversion efficiency to be ~0.15, using the approach of [6]. From the ChoCoLaT2 calculation we find that the target charge is 27 nC, the target charging process lasts ~10 ps, and the radius of the hot electron spot inside the target is much larger than the laser spot. On this basis we set the input for CST S2 simulation as follows: electron bunches comprising 13.5 nC of charge are emitted on each side of the foil from a spot of 1.3 mm radius, with 30° ejection half-angle, with Gaussian temporal profile having 5.5 ps FWHM. Due to constraints of the CST S2 package we had to assume that electrons are ejected with nearly uniform energy, which was set to 160 keV by trial-and-error method to avoid excessive early quasi-particle absorption on conducting surfaces. Results of simulations for the target on a Cu stalk (1.5 mm radius, 25 mm height) placed on a 24×10×50 mm Al pedestal grounded at the bottom are shown in Fig. 1, where the component of the H-field perpendicular to the laser-axis-target-stalk plane is displayed. We see that at later times the contribution from the neutralization current oscillating in the target stalk is clearly visible, consistently with the picture outlined in [7]. However, in the very early stage the EMP signal is dominated by a very strong pulse originating directly from the laser-target interaction point, which has no relation to the neutralization current.

In a second step, this simulation was repeated with the Cu stalk replaced by a dielectric stalk. The result is rather simple: the initial strong EMP signal originating from the laser-target interaction point is still present, but instead of the oscillating current discharge that followed in the case of the metal stalk we have a gradual discharge over the period of few ns. The final simulated configuration was that of a target foil placed in a metal box – dubbed “birdhouse” – either on a metal crossbar connected to resistors or on a dielectric crossbar. The birdhouse in this case was an Al box with dimensions 32×22×34 mm, with two holes 8 mm in diameter for the laser beam input and for the accelerated ion output, placed on the same Al pedestal as the metal stalk target. The pattern of the EMP emission for such target is shown in Fig. 2. We see that the initial strong pulse emitted from the laser-target interaction point is mostly confined within the box, and the dominant EMP emission occurs at much lower wavelengths than in the case of the target on a metal stalk. This confirms the expectation that the birdhouse target would be effective in mitigating the EMP emission in low-GHz frequency range [4].

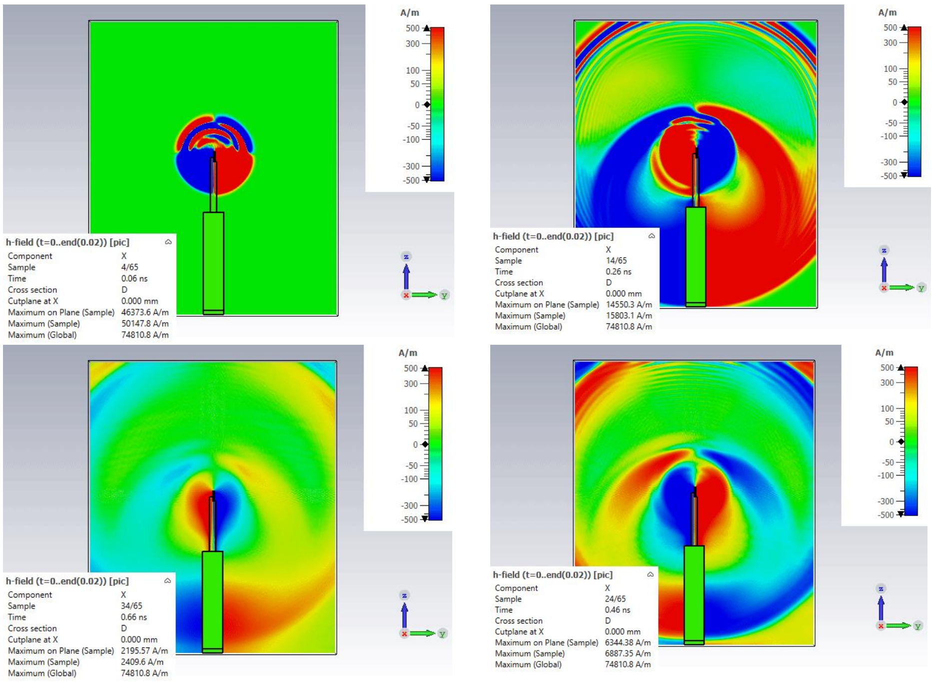

```
h-field (t=0..end(0.02)) [pic]
Component                   X
Sample                      4/65
Time                        0.06 ns
Cross section               D
Cutplane at X               0.000 mm
Maximum on Plane (Sample)   46373.6 A/m
Maximum (Sample)            50147.8 A/m
Maximum (Global)            74810.8 A/m
```

```
h-field (t=0..end(0.02)) [pic]
Component                   X
Sample                      14/65
Time                        0.26 ns
Cross section               D
Cutplane at X               0.000 mm
Maximum on Plane (Sample)   14550.3 A/m
Maximum (Sample)            15803.1 A/m
Maximum (Global)            74810.8 A/m
```

```
h-field (t=0..end(0.02)) [pic]
Component                   X
Sample                      34/65
Time                        0.66 ns
Cross section               D
Cutplane at X               0.000 mm
Maximum on Plane (Sample)   2195.57 A/m
Maximum (Sample)            2409.6 A/m
Maximum (Global)            74810.8 A/m
```

```
h-field (t=0..end(0.02)) [pic]
Component                   X
Sample                      24/65
Time                        0.46 ns
Cross section               D
Cutplane at X               0.000 mm
Maximum on Plane (Sample)   6344.38 A/m
Maximum (Sample)            6887.35 A/m
Maximum (Global)            74810.8 A/m
```

Figure 1 The evolution of the H-field component perpendicular to the laser-axis-target-stalk plane, shown at 0.06 ns, 0.26 ns, 0.46 ns and 0.66 ns after the start of fast electron emission, for target foil mounted on a Cu stalk fitted on Al pedestal.

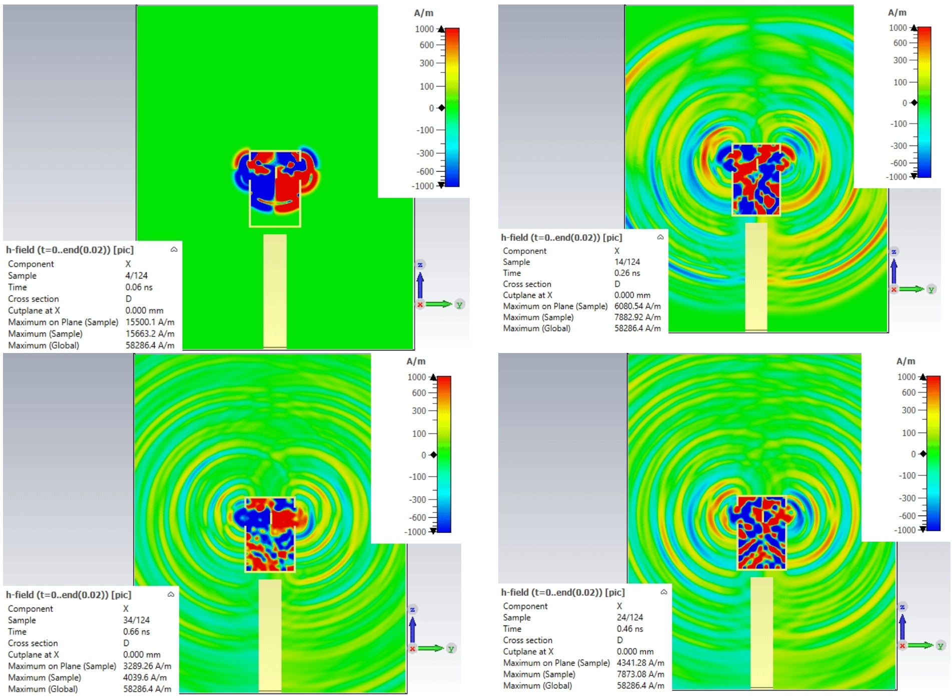

```
h-field (t=0..end(0.02)) [pic]
Component                   X
Sample                      4/124
Time                        0.06 ns
Cross section               D
Cutplane at X               0.000 mm
Maximum on Plane (Sample)   15500.1 A/m
Maximum (Sample)            15663.2 A/m
Maximum (Global)            58286.4 A/m
```

```
h-field (t=0..end(0.02)) [pic]
Component                   X
Sample                      14/124
Time                        0.26 ns
Cross section               D
Cutplane at X               0.000 mm
Maximum on Plane (Sample)   6080.54 A/m
Maximum (Sample)            7882.92 A/m
Maximum (Global)            58286.4 A/m
```

```
h-field (t=0..end(0.02)) [pic]
Component                   X
Sample                      34/124
Time                        0.66 ns
Cross section               D
Cutplane at X               0.000 mm
Maximum on Plane (Sample)   3289.26 A/m
Maximum (Sample)            4039.6 A/m
Maximum (Global)            58286.4 A/m
```

```
h-field (t=0..end(0.02)) [pic]
Component                   X
Sample                      24/124
Time                        0.46 ns
Cross section               D
Cutplane at X               0.000 mm
Maximum on Plane (Sample)   4341.28 A/m
Maximum (Sample)            7873.08 A/m
Maximum (Global)            58286.4 A/m
```

Figure 2 The evolution of the H-field component perpendicular to the laser-axis-target-stalk plane, shown at 0.06 ns, 0.26 ns, 0.46 ns and 0.66 ns after the start of fast electron emission, for the target foil mounted on a dielectric crossbar in an Al box.

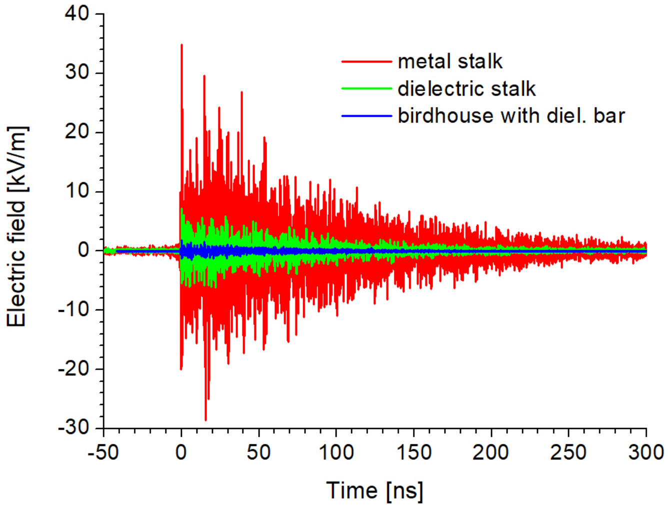

Figure 3 EMP amplitudes for three representative shots with target foils placed on a metal stalk (red line), dielectric stalk (green line) and in a birdhouse with a dielectric crossbar (blue line), measured 29 cm from the target at the laser-target interaction level. Significant reduction in the EMP amplitude with the birdhouse target is achieved.

Results of EMP simulations are consistent with the measurements performed at the IPPLM laser facility. In Fig. 3 we compare EMP amplitudes for three shots representative of a bigger sample, involving the target foil on a metal stalk, the foil on dielectric stalk and the foil placed in a birdhouse on a dielectric crossbar. Plots represent the vertical component of the electric field strength measured using the Prodyn FD5C probes 29 cm from the target, at the level of the laser-target interaction point. We see that the birdhouse target offers significant EMP reduction relative to both the metal stalk case and the dielectric stalk. The amplitude mitigation factor relative to the metal stalk is ~20, and the spectral mitigation factor in the frequency range near 1 GHz is ~40.

Our results confirm the observation that the birdhouse approach is a promising EMP mitigation approach. This approach should be particularly useful in experiments that require very low EMP signatures. Our simulations also show that EMP emission from various target may contain nontrivial contributions in the 10’s of GHz range, which should be taken into account in experiments aimed at EMP characterization on various systems. Our results also show that it is of interest to perform EMP measurements in correlation with proton acceleration measurements, since target charging and ion acceleration are ruled by similar physics.

References

[1] F. Consoli *et al.*, *High Pow Laser Sci Eng*, vol. 8, pp. e22, 1–59, 2020.
[2] A. V. Brantov *et al.*, *Phys. Rev. E*, vol. 102, no. 2, p. 021202, Aug. 2020.
[3] M. Bardon *et al.*, *Phys. Rev. Research*, vol. 2, no. 3, p. 033502, Sep. 2020.
[4] J. L. Dubois *et al.*, *Review of Scientific Instruments*, vol. 89, pp. 103301, 1–8, Oct. 2018.
[5] A. Poyé *et al.*, *Phys. Rev. E*, vol. 98, no. 3, pp. 033201, 1–12, Sep. 2018.
[6] P. Rączka *et al.*, *Acta Phys. Pol. A*, vol. 138, no. 4, pp. 593–600, Oct. 2020.
[7] J.-L. Dubois *et al.*, *Phys. Rev. E*, vol. 89, no. 1, pp. 013102, 1–15, Jan. 2014.